SUPPLEMENTARY MATERIALS

Figures S1 – S4

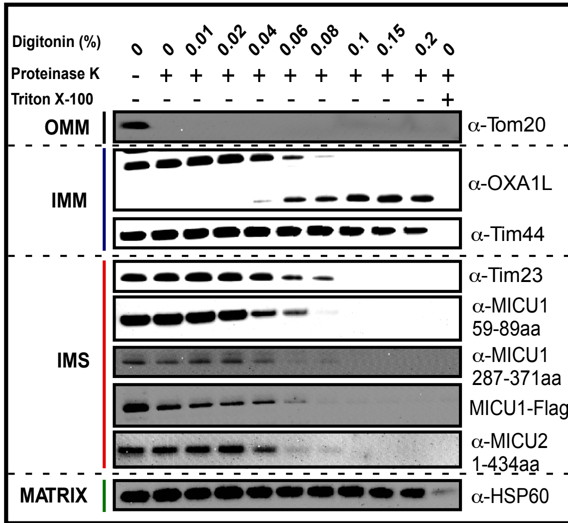

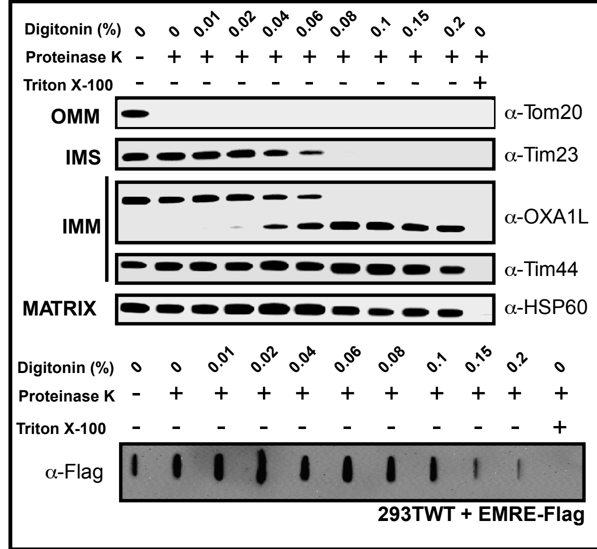

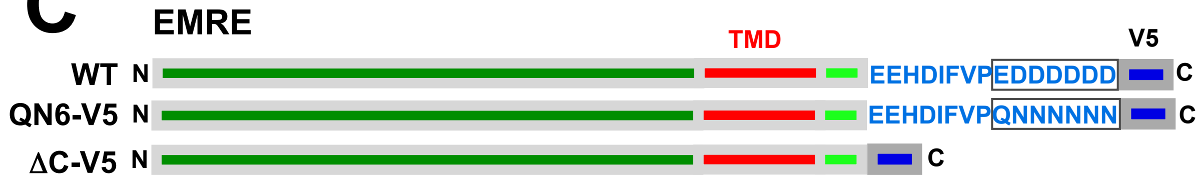

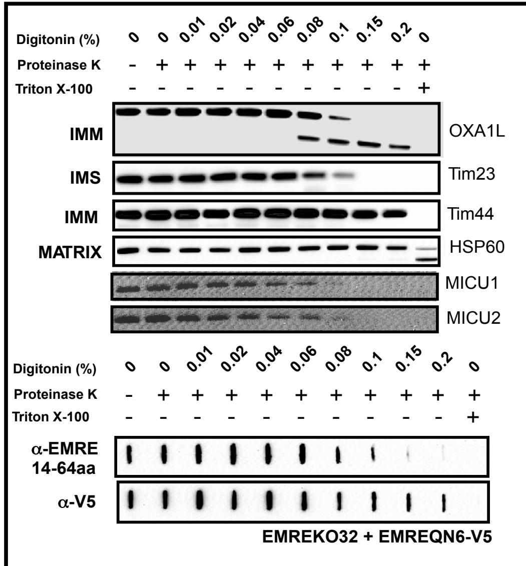

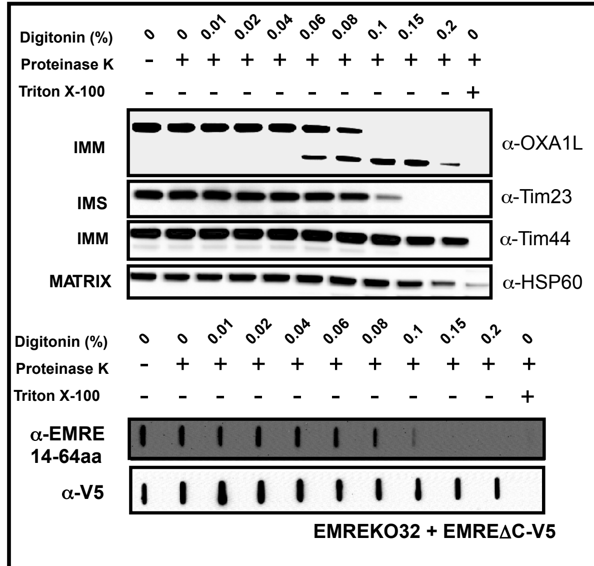

Figure S1

Figure S1. Related to Figure 2. **Proteinase sensitivity assays establishing the topology of MICU1, MICU2 and EMRE within the mitochondrion**

(A) MICU1 and MICU2 are facing the inter-membrane space (IMS). MICU1 localization was probed with three different antibodies, with specificities for different regions in the MICU1 sequence indicated.

(B) The flag-tagged carboxyl terminus of EMRE is facing the mitochondrial matrix (same as EMRE-V5, Fig. 2A).

(C) Schematic representations of V5-tagged EMRE-rescue, EMRE-ΔC and EMRE-QN6 constructs, used throughout the study.

(D) QN6 mutations of EMRE does not affect its topology or the IMS localization of MICU1 and MICU2.

(E) Truncation of the carboxyl terminus of EMRE does not alter its topology in the mitochondrion.

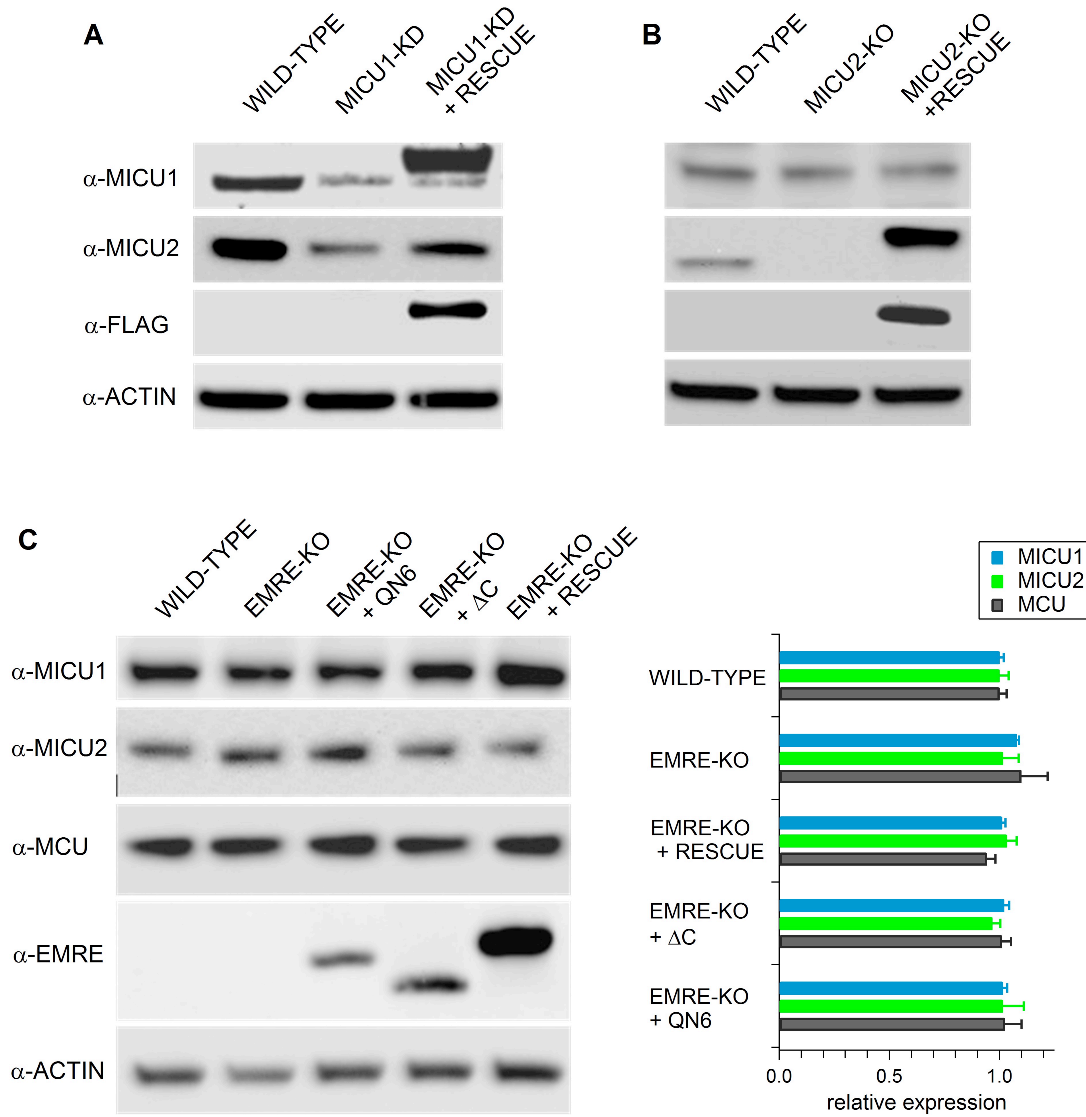

Figure S2 related to Figure 2. **Biochemical validation of cell lines**

(A) Western blots with MICU1-KD and MICU1-KD + rescue cells, showing expression levels of MICU1 and MICU2.

(B) Same as in (A) but with MICU2-KO and MICU2-KO + rescue cells.

(C) MICU1, MICU2 and MCU expression are the same as in the wild-type cells when either EMRE-rescue or its truncated/mutated forms are expressed in EMRE-KO cells. All EMRE constructs are expressed well above the wild-type level, which was not detected in these experimental conditions.

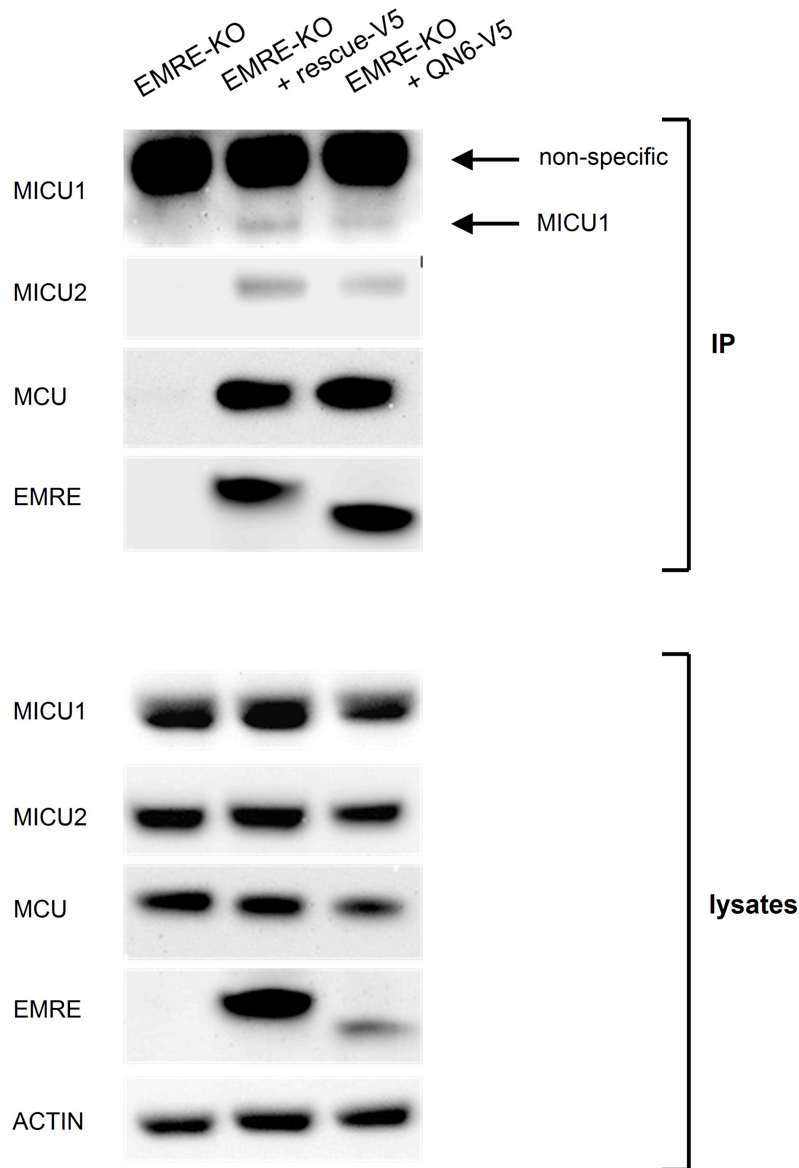

Figure S3

Figure S3 related to Figure 2. **Mutation of the C-terminus of EMRE (QN6) does not disrupt EMRE-MCU-MICU1-MICU2 complex formation**

EMRE was immunoprecipitated from HEK293 EMRE-KO cells, EMRE-KO cells rescued with WT V5-tagged EMRE (EMRE KO + rescue-V5) or V5-tagged EMRE-QN6 (EMRE-KO + QN6-V5) with anti-V5 agarose. Immunoprecipitates and lysates immunoblotted for indicated proteins.

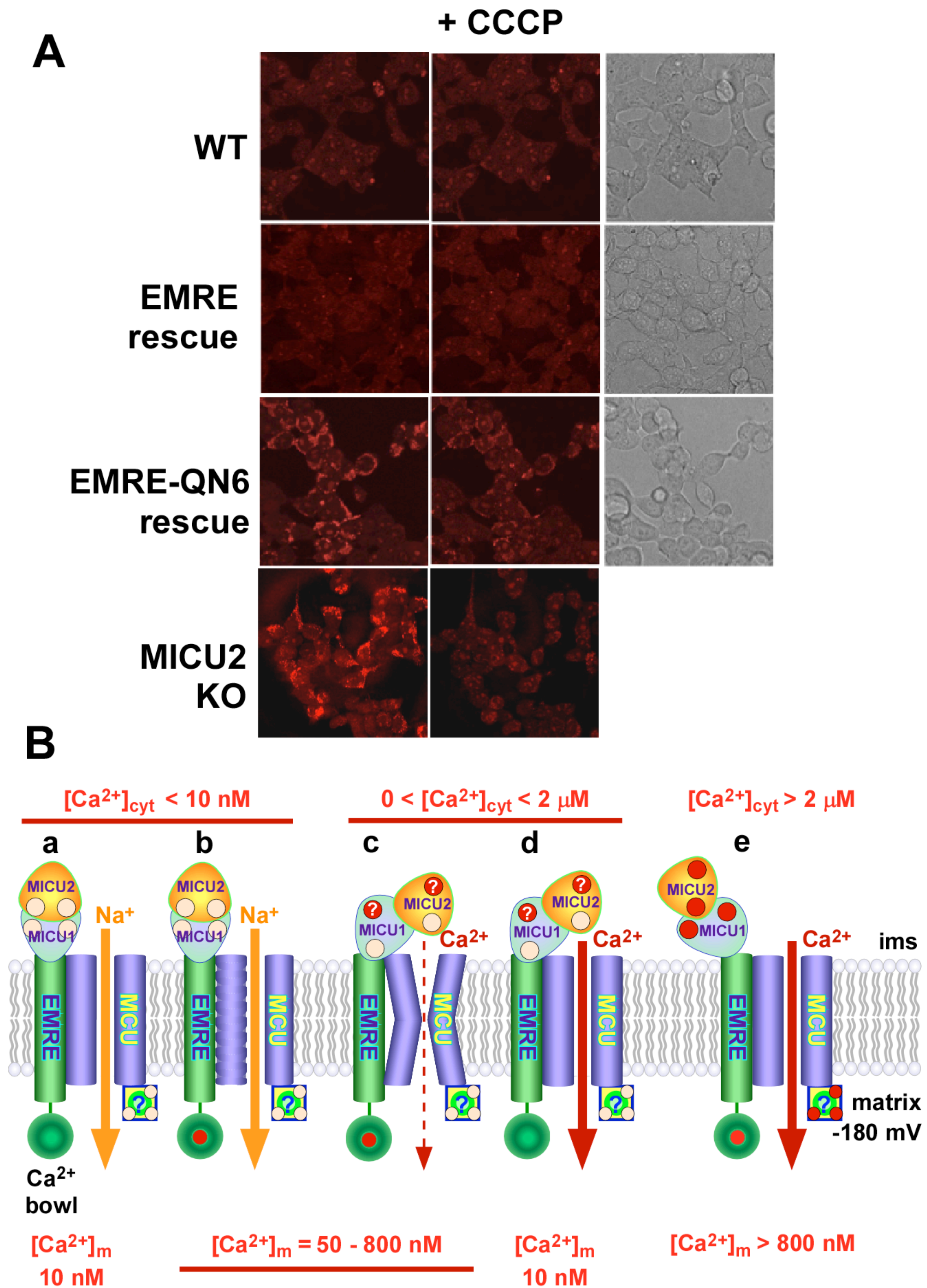

Figure S4

Figure S4 related to Figures 2-4**. Rhod-2 reports mitochondrial matrix [Ca^{2+}] and model for matrix and intermembrane space [Ca^{2+}] regulation of MCU activity.**

(A) Rhod-2 fluorescence imaged in different HEK cell lines, as indicated, in absence and after subsequent exposure to 5-10 µM CCCP. Elevated Rhod-2 fluorescence observed in EMRE-QN6 rescue cells and MICU2 KO cells was punctate and strongly reduced by CCCP, indicating that basal mitochondria [Ca2+] was elevated in this cells compared with WT cells.

(B) Model for MCU regulation, with Ca^{2+} sensors on both sides of the IMM: EMRE and an unknown protein (box associated with MCU in the cartoon) sense matrix [Ca^{2+}] ([Ca^{2+}]$_m$); MICU1 and/or MICU2, through their paired EF hands (red dots), represent intermembrane space (ims) cytoplasmic Ca^{2+} ([Ca^{2+}]$_{cyt}$) sensor(s). Under normal resting conditions channel open probability is strongly reduced (gatekeeping) when sensors on both sides of the IMM are liganded with Ca^{2+} (conformation **c**; red dots with question marks signify Ca^{2+} binding sites possibly liganded). Channel inhibition is effective in the range of [Ca^{2+}]$_m$ = 50-800 nM, with maximal inhibition at [Ca^{2+}]$_m$ ~ 400 nM (from I_{MiCa} biphasic matrix [Ca^{2+}] dependence with apparent inhibition constant of 60 nM and apparent recovery constant of 730 nM; Figure 1D) with peak inhibition of MCU currents by ~75% at ~400 nM, and [Ca^{2+}]$_{cyt}$ between resting levels and ~ 2 mM (from permeabilized cell measurements here and in (Mallilankaraman et al., 2012); conformation **c**, with MICU proteins shown with unknown number of their EF hands liganded with Ca^{2+}; 25% open probability indicated by dashed line). Physiological relief of MCU channel inhibition is achieved by agonist-induced elevated [Ca^{2+}]$_{cyt}$ that drives Ca^{2+} into the matrix, raising [Ca^{2+}]$_m$ to levels (>800 nM) that result in highly cooperative activation (Hill coefficient > 3) of mitochondrial Ca^{2+} influx by unknown mechanisms (conformation **e**, with the unknown matrix reactivation mechanisms depicted as a Ca^{2+} binding protein with multiple Ca^{2+} binding sites, and MICU proteins with EF hands fully liganded). MCU channel inhibition can also be relieved by very low [Ca^{2+}]$_{cyt}$, independent of Ca^{2+} binding to EMRE (conformations **a** and **b**) and by low [Ca^{2+}]$_m$, independent of the Ca^{2+} binding state of MICU proteins (conformation **d**).